

Electronic Supplementary Information for

**Tuned Lifetime of a Xanthenic Fluorescent Dye by Means of
Buffer-Mediated Excited-State Proton Exchange Reaction.
Implications on Fluorescence Correlation Spectroscopy.**

Jose M. Paredes, Luis Crovetto, Ramon Rios[†], Angel Orte, Jose M. Alvarez-Pez^{*}, Eva
M. Talavera

*Department of Physical Chemistry, University of Granada, Cartuja Campus, Granada
18071, Spain.*

*[†]Current address: ICREA Researcher at Department of Organic Chemistry, University
of Barcelona. 08028 Barcelona, Spain*

**Author to whom correspondence should be addressed.*

Tel.: + 34-958-243831; fax: + 34-958-244090; e-mail: jalvarez@ugr.es

TABLE OF CONTENTS

¹ H NMR data of 9-[1-(2-Methyl-4-methoxyphenyl)]-6-hydroxy-3H-xanthen-3-one (TG-II).	3
Influence of ionic strength on the ground-state acidity constant.	3
ESPT Reaction. Steady-State Emission Spectra.....	4
Theory of the global bicompartamental analysis.....	5
Program implementation and data analysis of time-resolved fluorescence.....	8
Details on the fitting of the fluorescence decay surface of TG-II.....	10
References.....	12
Scheme S-1.....	13
Figure S1.....	14
Figure S2.....	15
Figure S3.....	16
Figure S4.....	17
Figure S5.....	18
Figure S6.....	19
Figure S7.....	20
Figure S8.....	21

¹H NMR of 9-[1-(2-Methyl-4-methoxyphenyl)]-6-hydroxy-3H-xanthen-3-one (TG-II).

¹H NMR (300 MHz, CD₃OD): δ 2.03 (s, 3H), 3.93 (s, 3H), 7.06 (dd, 1H, J = 2.2, 8.4 Hz), 7.11 (d, 1H, J = 2.0 Hz), 7.21 (dd, 2H, J = 2.2, 9.2 Hz), 7.24 (d, 1H, J = 7.5 Hz), 7.32 (d, 2H, J = 2.2 Hz), 7.61 (d, 2H, J = 9.3 Hz). ¹³C NMR (75 MHz, CD₃OD): δ 20.16, 56.02, 103.56, 112.97, 117.38, 118.49, 121.54, 124.60, 131.90, 134.61, 139.24, 161.07, 163.19, 167.58, 173.20. MS (EI⁺): *m/z* 332 (M⁺). HRMS (ESI⁺): *m/z* calcd for (M + H)⁺, 333.11268; found, 333.10856. Yield: 89%.

Influence of ionic strength on the ground-state acidity constant.

Application of the Hendersson-Hasselbalch equation to the studied equilibrium of TG-II at near-physiological pH provides:^{S1,S2}

$$\text{p}K_{\text{a}}^{\text{app}} = \text{p}K_{\text{a}} + \log\left(\frac{f_{\text{A}}}{f_{\text{N}}}\right) - \log(a_{\text{H}_2\text{O}}) \quad (\text{S-1})$$

where f_{N} and f_{A} denote the activity coefficients of the neutral and the anion of TG-II, respectively, and $a_{\text{H}_2\text{O}}$ is the water activity. Since (N) can be an electrically neutral quinoid structure or a double electrically charged structure, its activity coefficient f_{N} at low ionic strength would be approximate to 1 or lower than 1, respectively.

A semi-empirical function based on the extended Debye-Hückel equation could be used to relate f_i with μ . Using this approach the activity coefficients may be represented as:

$$\log f_i = \frac{-A_{\text{DH}} z_i^2 \sqrt{\mu}}{1 + a_i B \sqrt{\mu}} + L_i \mu \quad (\text{S-2})$$

In this equation, also called the Truesdell-Jones equation, L_i is an adjustable parameter, typical values for A_{DH} and B at room temperature and atmospheric pressure are 0.51 and 0.33, respectively, \dot{a}_i stands for the ionic radius in Angstroms, and z_i is the ionic charge. Substituting eq S-1 into S-2, and assuming a similar radius for N and A (i.e., $\dot{a}_N = \dot{a}_A = \dot{a}$), leads to eq S-3:

$$\text{p}K_a^{\text{app}} = \text{p}K_a - \left(A_{DH} (z_A^2 - z_N^2) \frac{\sqrt{\mu}}{1 + \dot{a} B \sqrt{\mu}} + L^* \mu \right) - \log(a_{H_2O}) \quad (\text{S-3})$$

Since the experimental molecular radius of TG-II is not available, we have built a model of the molecule using the Sybyl program^{S3} to calculate the size and the molecular radius of the TG-II compound. To this purpose, appropriate fragments from the Sybyl libraries were used to build the molecule, and partial atomic charges were calculated by means of the Gasteiger-Marsili method.^{S4} The Tripos force field^{S5} was used in the energy calculation and the geometry was optimized using the Powel method,^{S6} until the energy gradient was smaller than 0.05 kcal mol⁻¹ Å². Figure S5 represents the optimized geometry of TG-II, as well as some significant distances in the anionic form of the molecule. These distances between the center of mass (C-7) and some distal points of the molecule range from 5.5 to 6.5 Å, in good agreement with the average value of 6.3 Å used in the fitting.

ESPT Reaction. Steady-State Emission Spectra.

In Figure S6a the fluorescence spectra from aqueous TG-II solutions in the presence of different concentrations of phosphate buffer in the range between 0.002 and 1.00 M, at pH 6.80, are shown. As can be seen, increasing the phosphate buffer

concentration resulted in a pronounced decrease in the intensities of the emission band, and this quenching effect saturated around 1.0 M phosphate buffer. At the experimental conditions, with pH values higher than ground state pK_a and 490 nm wavelength, the much more fluorescent TG-II anion is excited, then the buffer-mediated ESPT reaction rapidly occurs during its excited lifetime forming the non fluorescent neutral form, and the decay of the two species becomes coupled. Since the neutral form is not fluorescent and the pH-dependent coupled decay is characterized by a shorter lifetime than that of the anion, the system presents lower steady-state fluorescence intensity. For this model the normalized fluorescence intensity can be expressed by^{S7}

$$\frac{I}{A} = \frac{\phi_1}{1 + 10^{(pH - pK_a^*)}} + \frac{\phi_2}{1 + 10^{(pK_a^* - pH)}} \quad (\text{S-4})$$

where I/A is the fluorescence intensity at λ_{em} , normalized by absorbance at the excitation wavelength, ϕ_1 and ϕ_2 are the relative fluorescence efficiencies of the neutral and anion at λ_{em} , and pK_a^* is the pK_a for the excited-state proton reaction $1^* \rightleftharpoons 2^* + H^+$.

Theory of the global bicompartamental analysis.

When exciting the photophysical system shown in Scheme 2 with a δ -pulse at time $t = 0$, that does not significantly alter the concentrations of the ground-state species, the time course of the concentrations of the excited-state species 1^* and 2^* is described by the first-order differential equation

$$\dot{\mathbf{x}}(t) = \mathbf{A}\mathbf{x}(t) \quad (\text{S-5})$$

$\mathbf{x}(t)$ is the 2×1 vector function of the concentrations of the excited-state species 1^* and 2^* :

$$\begin{pmatrix} x_1(t) \\ x_2(t) \end{pmatrix} = \begin{pmatrix} [1^*](t) \\ [2^*](t) \end{pmatrix} \quad (\text{S-6})$$

$\dot{\mathbf{x}}(t)$ denotes its time derivative and \mathbf{A} is the 2×2 compartmental matrix:

$$\mathbf{A} = \begin{bmatrix} -(k_{01} + k_{21} + k_{21}^b[\text{R}]) & k_{12}[\text{H}^+] + k_{12}^b[\text{HR}] \\ k_{21} + k_{21}^b[\text{R}] & -(k_{02} + k_{12}[\text{H}^+] + k_{12}^b[\text{HR}]) \end{bmatrix} \quad (\text{S-7})$$

The fluorescence impulse response function, $f(\lambda_{\text{em}}, \lambda_{\text{ex}}, t)$, at emission wavelength λ_{em} due to excitation at λ_{ex} is given by eq. S-8,^{S8} and depends on λ_{ex} , λ_{em} , $[\text{H}^+]$, and the total buffer concentration ($C^{\text{B}} = [\text{R}] + [\text{HR}]$)

$$f(\lambda_{\text{em}}, \lambda_{\text{ex}}, t) = \kappa \tilde{\mathbf{c}} \mathbf{U} \exp(\mathbf{\Gamma} t) \mathbf{U}^{-1} \tilde{\mathbf{b}} \quad (\text{S-8})$$

In this equation, we assume that the 2×2 compartmental matrix \mathbf{A} has two linearly independent eigenvectors \mathbf{U}_1 and \mathbf{U}_2 associated with the eigenvalues γ_1 and γ_2 , respectively, i.e. $\mathbf{A} = \mathbf{U} \mathbf{\Gamma} \mathbf{U}^{-1}$ with $\mathbf{U} = [\mathbf{U}_1, \mathbf{U}_2]$ and \mathbf{U}^{-1} the inverse of the matrix of the eigenvectors, $\mathbf{\Gamma}$ is the diagonal matrix of two eigenvalues, and $\exp(\mathbf{\Gamma} t) = \text{diag}[\exp(\gamma_1 t), \exp(\gamma_2 t)]$. \mathbf{U} and $\exp(\mathbf{\Gamma} t)$ are functions of the rate constants k_{ij} and the concentrations $[\text{R}]$, $[\text{HR}]$, and $[\text{H}^+]$.

The concentrations of species i^* at time zero are defined by $\mathbf{x}(0) = \mathbf{b}$ where \mathbf{b} is the 2×1 vector with elements b_i ($i = 1, 2$). \mathbf{b} depends on the excitation wavelength λ_{ex} and $[\text{H}^+]$. $\tilde{\mathbf{b}}$ is the 2×1 vector with normalized elements of \mathbf{b} . The elements \tilde{b}_i are calculated by^{S8}

$$\tilde{b}_i = \frac{\varepsilon_i \alpha_i}{\sum_i \varepsilon_i \alpha_i} \quad (\text{S-9})$$

where ε_i is the molar absorption coefficient of the i^{th} compartment, and α_i the molar fraction of each form in the ground-state.

$\tilde{\mathbf{c}}$ is the 1×2 vector of the normalized emission weighting factors ($\tilde{c}_i = c_i / \sum_i c_i$) of species i^* at emission wavelength λ_{em} .^{S8}

$$c_i(\lambda_{\text{em}}) = k_{Fi} \int_{\Delta\lambda_{\text{em}}} \rho_i(\lambda_{\text{em}}) d\lambda_{\text{em}} \quad (\text{S-10})$$

where k_{Fi} is the fluorescence rate constant of i^* ; $\Delta\lambda_{\text{em}}$ is the emission wavelength interval around λ_{em} where the fluorescence signal is monitored; $\rho_i(\lambda_{\text{em}})$ is the emission density of i^* at λ_{em} defined by^{S8}

$$\rho_i(\lambda_{\text{em}}) = \frac{F_i(\lambda_{\text{em}}, \lambda_{\text{ex}})}{\int_{\text{full emission band}} F_i(\lambda_{\text{em}}, \lambda_{\text{ex}}) d\lambda_{\text{em}}} \quad (\text{S-11})$$

where the integration extends over the whole steady-state fluorescence spectrum F_i of species i^* .

Finally, κ is a proportionality constant given by

$$\kappa = \sum_{\forall_i} b_i \sum_{\forall_i} c_i \quad (\text{S-12})$$

The use of κ , \tilde{b}_i , and \tilde{c}_i allows one to link \tilde{b}_i and \tilde{c}_i in the data analysis so that the collected decay traces are not required to be scaled. Indeed, $\tilde{\mathbf{b}}$ depends on λ_{ex} and $[\text{H}^+]$ (or pH), whereas $\tilde{\mathbf{c}}(\lambda_{\text{em}})$ depends on the emission wavelength only. In the implementation of global compartmental analysis one fits directly for the rate constants k_{01} , k_{21} , k_{02} , k_{12} , k_{12}^b , k_{21}^b , the normalized zero-time concentrations \tilde{b}_1 of species $\mathbf{1}^*$, and the normalized spectral emission weighting factors $\tilde{c}_1(\lambda_{\text{em}})$ of species $\mathbf{1}^*$.

Eq. S-8 can be written in the common bi-exponential format (with $t \geq 0$):

$$f(t) = p_1 e^{\gamma_1 t} + p_2 e^{\gamma_2 t} \quad (\text{S-13})$$

The eigenvalues γ_i ($i = 1, 2$) of the compartmental matrix \mathbf{A} are related to the decay times τ_i ($i = 1, 2$) according to

$$\gamma_i = -1/\tau_i \quad (\text{S-14})$$

and are given by

$$\gamma_i = \frac{a_{11} + a_{22} \pm \sqrt{(a_{22} - a_{11})^2 + 4a_{12}a_{21}}}{2} \quad (\text{S-15})$$

with a_{ij} the ij^{th} element of the compartmental matrix \mathbf{A} (eq. S-7).

The pre-exponentials, p_i , of eq. S-13 are related to compartmental parameters through the following equations:

$$p_1 = \kappa(\tilde{c}_1\beta_{11} + \tilde{c}_2\beta_{21}) \quad (\text{S-16 a})$$

$$p_2 = \kappa(\tilde{c}_1\beta_{12} + \tilde{c}_2\beta_{22}) \quad (\text{S-16 b})$$

$$\beta_{11} = \frac{[\tilde{b}_1(\gamma_2 - a_{11}) - \tilde{b}_2a_{12}]}{(\gamma_2 - \gamma_1)} \quad (\text{S-17 a})$$

$$\beta_{12} = -\frac{[\tilde{b}_1(\gamma_1 - a_{11}) - \tilde{b}_2a_{12}]}{(\gamma_2 - \gamma_1)} \quad (\text{S-17 b})$$

$$\beta_{21} = \frac{[\tilde{b}_2(\gamma_2 - a_{22}) - \tilde{b}_1a_{21}]}{(\gamma_2 - \gamma_1)} \quad (\text{S-17 c})$$

$$\beta_{22} = -\frac{[\tilde{b}_2(\gamma_1 - a_{22}) - \tilde{b}_1a_{21}]}{(\gamma_2 - \gamma_1)} \quad (\text{S-17 d})$$

Program implementation and data analysis of time-resolved fluorescence.

The global compartmental analysis of the collected fluorescence decay surfaces was implemented in a general global analysis program using Gaussian-weighted non-linear

least-squares fitting based on Marquardt-Levenberg minimization.^{S9} Its first description and application was done at the system fluorescein-(±)-N-acetyl aspartic acid.^{S10}

Consider the excited-state process in the presence of added buffer as depicted in Scheme 2. The parameters were linked as shown in Scheme S-1. The global (linkable) fitting parameters are k_{01} , k_{02} , k_{21} , k_{12}^B , k_{21}^B , \tilde{b}_1 , and \tilde{c}_1 . The rate constants k_{ij} are independent of λ_{ex} , λ_{em} , and pH, and hence can be linked over the entire fluorescence decay data surface. The emission weighting factors \tilde{c}_1 only depend on λ_{em} and therefore can be linked at the same emission wavelength. The spectral parameters \tilde{b}_1 are dependent on both λ_{ex} and pH and consequently can only be linked at the same λ_{ex} and pH. The only local (nonlinkable) fitting parameters are the scaling factors κ .

At each pH and C^B , the values of [R] and [HR] of the buffer with acidity constant K_a^B were computed according to:

$$[\text{R}] = \frac{K_a^B C^B}{K_a^B + [\text{H}^+]} \quad (\text{S-18 a})$$

$$[\text{HR}] = \frac{[\text{H}^+] C^B}{K_a^B + [\text{H}^+]} \quad (\text{S-18 b})$$

Assigning initial guesses to the rate constants k_{01} , k_{02} , k_{21} , k_{12}^B , and k_{21}^B allows one to construct the compartmental matrix **A** (eq. S-7) for each decay trace. The eigenvalues γ and the associated eigenvectors of this matrix are determined using routines from EISPACK, Matrix Eigensystem Routines.^{S11} The eigenvectors are then scaled to the initial conditions $\tilde{\mathbf{b}}$. The fluorescence δ -response of the sample, $f(\lambda^{\text{ex}}, \lambda^{\text{em}}, t)$ is calculated according eq. S-8. Then $f(\lambda^{\text{ex}}, \lambda^{\text{em}}, t)$ is convoluted with the experimental

instrument response function and the adjustable parameters of this calculated curve are optimized to fit the experimental fluorescence decay of the sample. Using this approach, experiments done at different excitation/emission wavelengths, at multiple timing calibrations, and at different pH are linked by all rate constants defining the system. The starting value for all rate constants k_{ij} was $1 \times 10^9 \text{ (M}^{-1} \text{ s}^{-1})$; for \tilde{b}_1 and \tilde{c}_1 , the initial guesses were 0 and/or 1. The generalized global mapping table approach described previously allows one to analyze simultaneously experiments done at different λ_{ex} and λ_{em} , at multiple timing calibrations, and at different pH and C^{B} values.

The fitting parameters were determined by minimizing the global *reduced* chi-square χ_g^2 :

$$\chi_g^2 = \sum_l^q \sum_i w_{li} (y_{li}^o - y_{li}^c)^2 / \nu \quad (\text{S-19})$$

where the index l sums over q experiments, and the index i sums over the appropriate channel limits for each individual experiment. y_{li}^o and y_{li}^c denote respectively the experimental and fitted values corresponding to the i th channel of the l th experiment, and w_{li} is the corresponding statistical weight. ν represents the number of degrees of freedom for the entire multidimensional fluorescence decay surface.

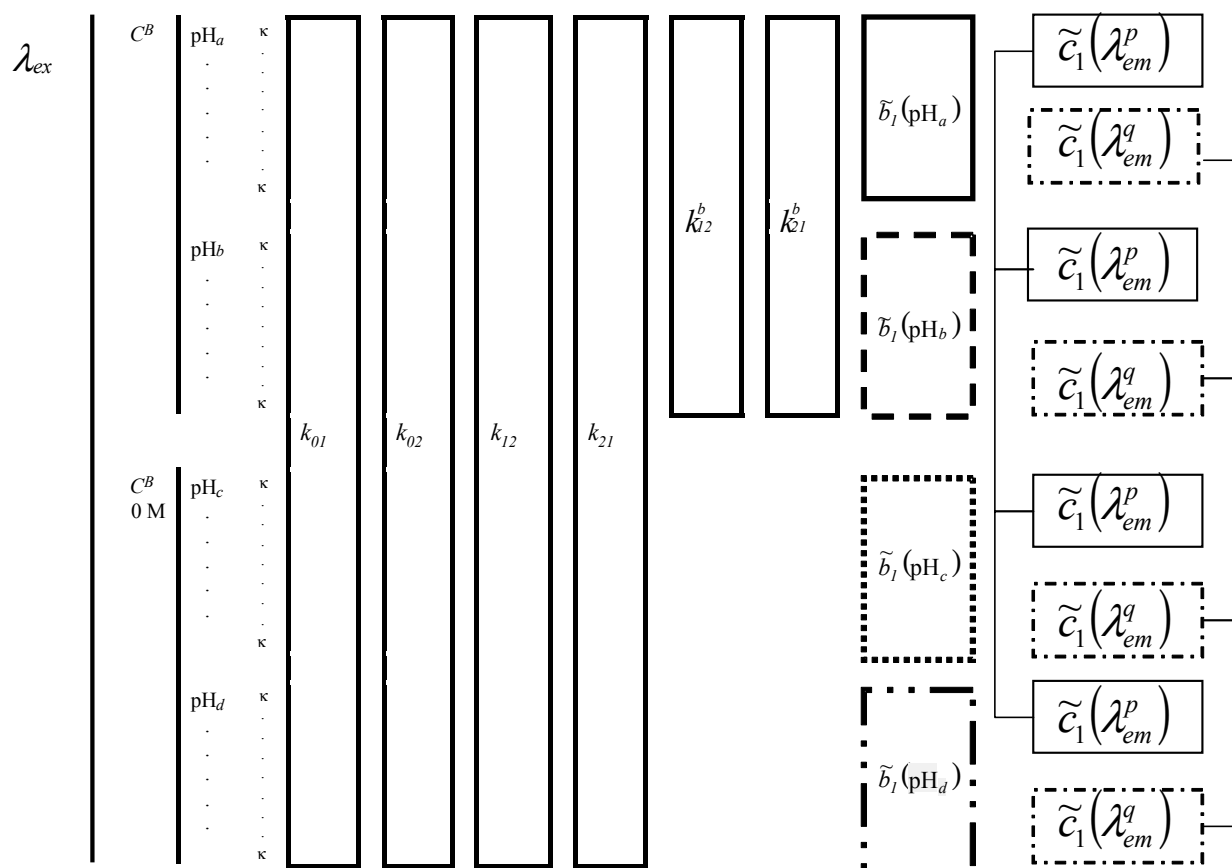
The goodness-of-fit was judged for each fluorescence decay trace separately as well as for the global fluorescence decay surface. The statistical criteria to assess the quality of the fit comprised both graphical and numerical tests, and have been described elsewhere.^{S12}

Details on the fitting of the fluorescence decay surface of TG-II.

As has been indicated in the article text, 90 selected decay traces at different pH values within the range 4.50-6.10 were recorded. Excitation wavelength was 488 nm, and emission wavelengths were 505, 515, and 535 nm. The fitting process finished with a $\chi^2 = 1.17$, and the final results did not depend on the initial guesses of the parameters. Visual adjustment of calculated decay functions, weighted residuals plot, and autocorrelation function plots were also used as goodness-of-fitting criteria. Figure S-7 shows two (mono- and biexponential) experimental decay traces, and the fitting curves provided by the GCA results (convoluted with the instrumental profile, shown as well in the figures).

REFERENCES

- [S1] Boens, N.; Qin, W.; Basarić, N.; Orte, A.; Talavera, E. M.; Alvarez-Pez, J. M. *J. Phys. Chem. A* **2006**, *1109*, 9334-9343.
- [S2] Crovetto, L.; Paredes, J. M.; Rios, R.; Talavera, E. M.; Alvarez-Pez, J. M. *J. Phys. Chem. A* **2007**, *111*, 13311-13320.
- [S3] SYBYL Molecular Modelling Software is available from Tripos Inc., 1699 S. Hanley Road, St. Louis, MO 63144-2913, <http://www.tripos.com>
- [S4] ^aGasteiger, J.; Marsili, M. *Tetrahedron* **1980**, *36*, 3219-3222. ^bGasteiger, J.; Marsili, M. *Org. Magn. Reson.* **1981**, *15*, 353-360.
- [S5] Clark, M.; Cramer, R. D. III; Van Opdenbosch, N. *J. Comput. Chem.* **1989**, *10*, 982-1012.
- [S6] Powell, M. J. D. *Math. Prog.* **1977**, *12*, 241-254.
- [S7] Yguerabide, J.; Talavera, E.; Alvarez, J.M.; Quintero, B. *Photochem. Photobiol.* **1994**, *60*, 435-441.
- [S8] Ameloot, M.; Boens, N.; Andriessen, R.; Van den Bergh, V.; De Schryver, F. C. *J. Phys. Chem.* **1991**, *95*, 2041-2047.
- [S9] Program developed jointly by the Technology Institute of the Belarusian State University (Minsk, Belarus) and the Division of Photochemistry and Spectroscopy of the K. U. Leuven (Leuven, Belgium).
- [S10] Crovetto, L.; Orte, A.; Talavera, E. M.; Alvarez-Pez, J. M.; Cotlet, M.; Thielemans, J.; De Schryver, F. C.; Boens, N. *J. Phys. Chem. B* **2004**, *108*, 6082-6092.
- [S11] Smith B. T.; Boyle J. M.; Garbow B. S.; Ikeke Y.; Klema V. C.; Moler C. B. in *Lecture Notes in Computer Science*, Goos, G.; Hartmanis, J., Eds.; Springer Verlag: Heidelberg, New York, 1974; Volume 6.
- [S12] Van den Zegel, M.; Boens, N.; Daems, D.; De Schryver, F. C. *Chem. Phys.* **1986**, *101*, 311-335.



Scheme S1. Linking scheme for the global compartmental analysis. Decays recorded at different emission wavelengths ($\tilde{c}_1(\lambda_{em}^p)$, $\tilde{c}_1(\lambda_{em}^q)$), due to a single excitation wavelength (λ_{ex}), and in the absence ($C^B = 0$) and the presence (C^B) of buffer. Boxed and/or connected parameters in the same line type indicate linked parameters, whereas κ denotes the local scaling factors. The rate constants k_{ij} are linked over the entire surface, whereas k_{ij}^b are only linked over decays in the presence of proton acceptor/donor. Excitation parameters \tilde{b}_1 are linked at the same pH value, and emission parameters \tilde{c}_1 are linked at the same emission wavelength.

Electronic Supplementary Material for PCCP

This Journal is © The Owner Societies

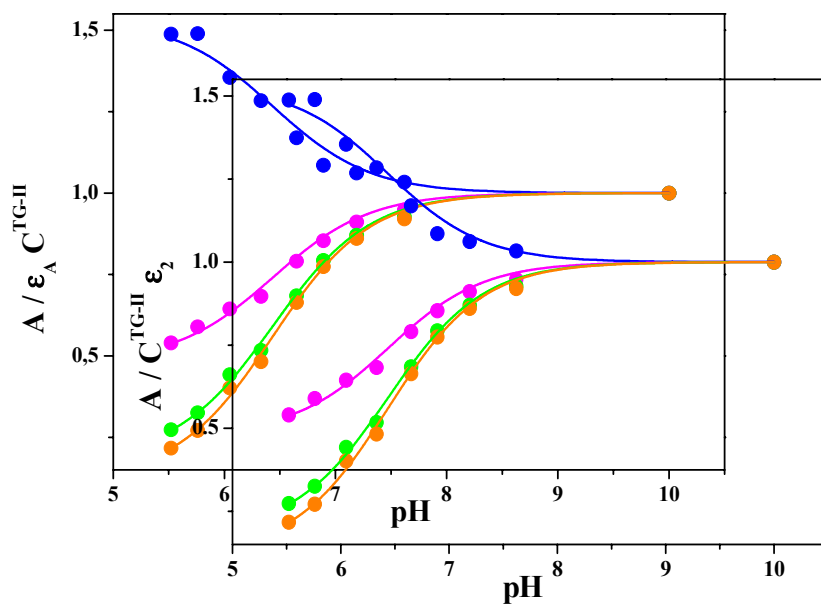


Figure S1. Global fitting of the $A/C^{\text{TG-II}} \epsilon_A$ vs. pH from experimental spectra of Fig. 1b, to the Beer's law and acid-base equilibrium equations. The fitted λ_{abs} were: (●) 440 nm, (●) 475 nm, (●) 490 nm and (●) 500 nm.

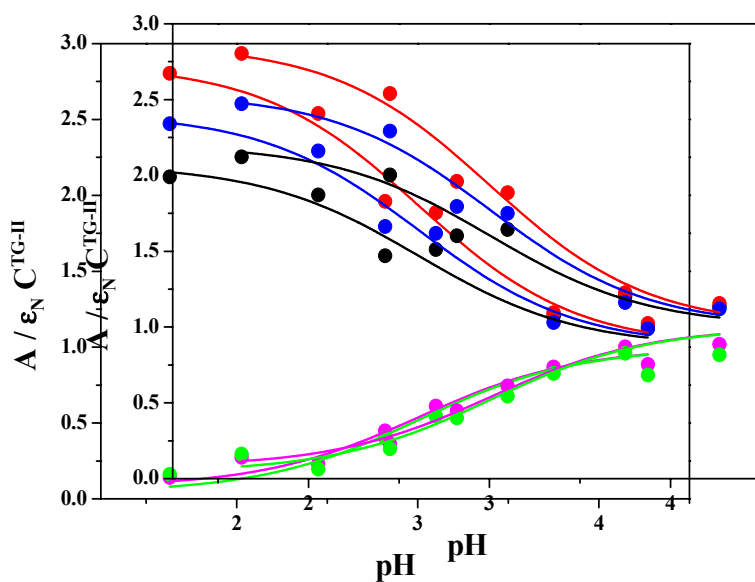


Figure S2. Global fitting of the $A/C^{\text{TG-II}} \epsilon_N$ vs. pH from experimental absorbance data, to the Beer's law and acid-base equilibrium equations. The fitted λ_{abs} were: (●) 400 nm, (●) 420 nm, (●) 440 nm, (●) 475 nm and (●) 490 nm.

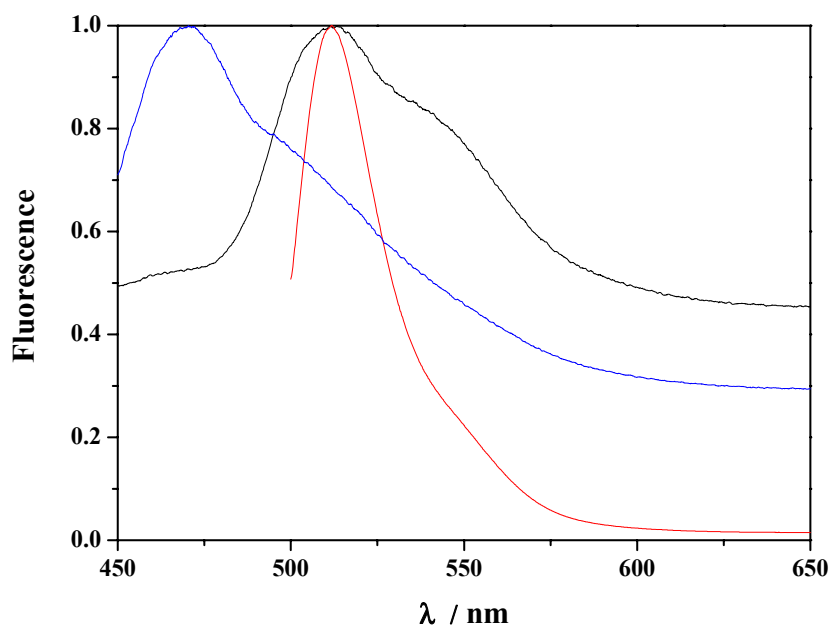


Figure S3. Normalized emission spectra of TG-II aqueous solutions at different pH values: (—) pH = 10.00; (—) pH = 1.63; (—) 7.0 M HClO₄. The emission spectrum at pH 10.00 was recorded at $\lambda_{\text{ex}} = 490$ nm and corresponds to the anion. Both emission spectra at pH 1.63 and 7.0 M HClO₄ were recorded at $\lambda_{\text{ex}} = 440$ nm. These spectra correspond respectively to the neutral and cation. It is noticeable that the fluorescence intensities of the spectra corresponding to the neutral and cation forms are very low, and the normalization was achieved by multiplying by a factor larger than 100.

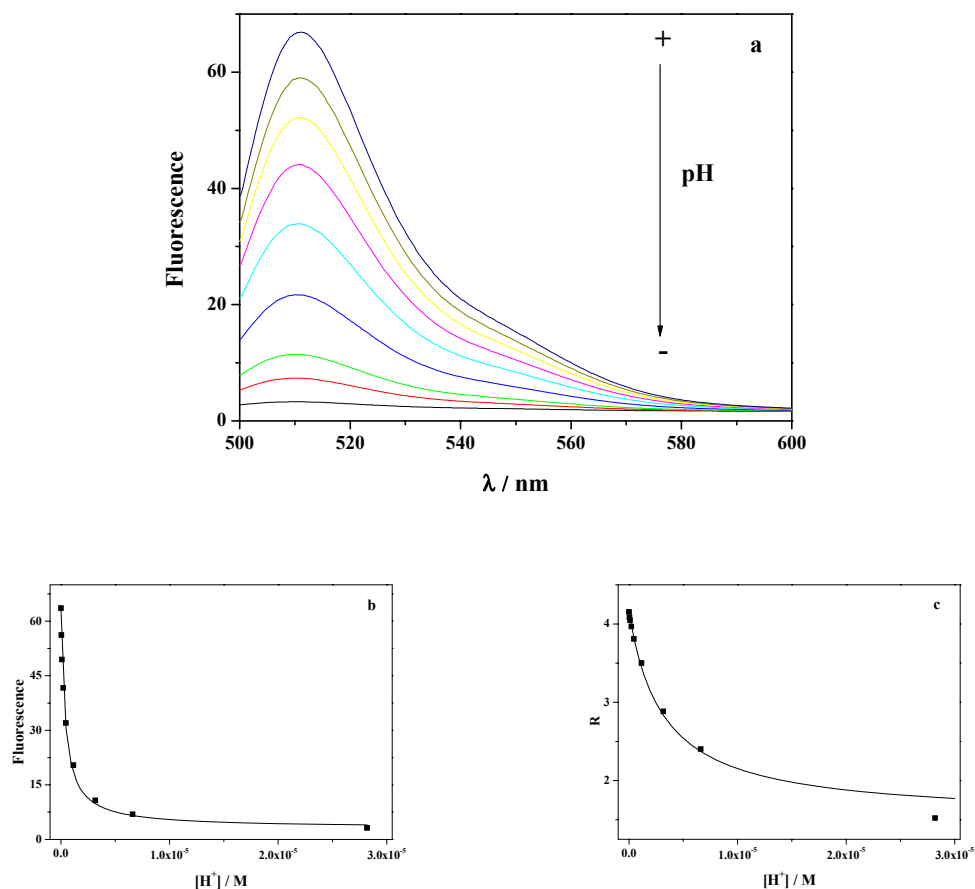


Figure S4. (a) Fluorescence emission spectra ($\lambda_{\text{ex}} = 490 \text{ nm}$) of TG-II $4 \times 10^{-6} \text{ M}$ in 0.01 M phosphate buffer with addition of 0.1 M KCl, at the following pH values: 4.55, 5.18, 5.5, 5.94, 6.35, 6.67, 7.00, 7.41, and 9.36. The arrow indicates decreasing pH values. **(b)**

Best fit of $F(\lambda_{\text{ex}}, \lambda_{\text{em}}, [\text{H}^+]) = \frac{F_{\text{max}} [\text{H}^+]^n + F_{\text{min}} K_a}{K_a + [\text{H}^+]^n}$ with $n = 1$ (solid line), to the *direct*

emission fluorimetric titration data from the spectra of Figure S3a (■) ($\lambda_{\text{ex}} = 490 \text{ nm}$, λ_{em}

$= 515 \text{ nm}$). **(c)** Best fit of $R = \frac{R_{\text{max}} [\text{H}^+]^n + R_{\text{min}} K_a \xi}{K_a \xi + [\text{H}^+]^n}$ (solid line) to the *ratiometric*

emission fluorimetric titration data from the spectra of Figure S3a (■).

$\xi = F_{\text{min}}(\lambda_{\text{ex}}, \lambda_{\text{em}}^2) / F_{\text{max}}(\lambda_{\text{ex}}, \lambda_{\text{em}}^2)$, ($\lambda_{\text{ex}} = 490 \text{ nm}$, $\lambda_{\text{em}}^1 = 515 \text{ nm}$, $\lambda_{\text{em}}^2 = 550 \text{ nm}$).

Electronic Supplementary Material for PCCP

This Journal is © The Owner Societies

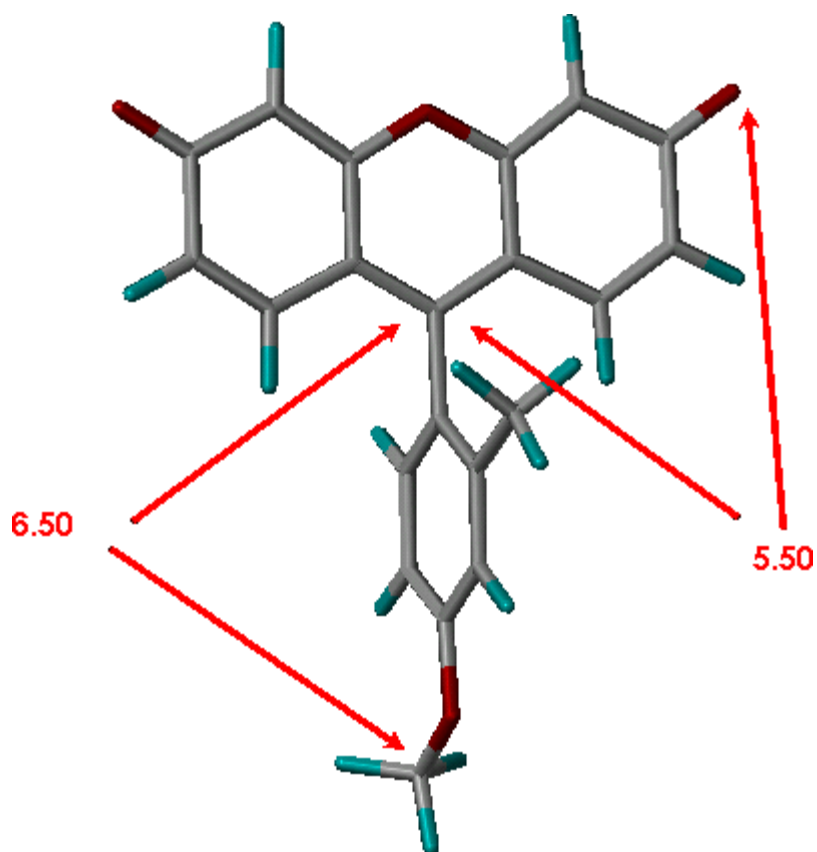


Figure S5. Optimized geometry of **TG-II** by means of the Sybyl programs. Arrows indicate distances measured between the center of mass of the molecule (that almost coincides with C7) and some distal points of the molecule.

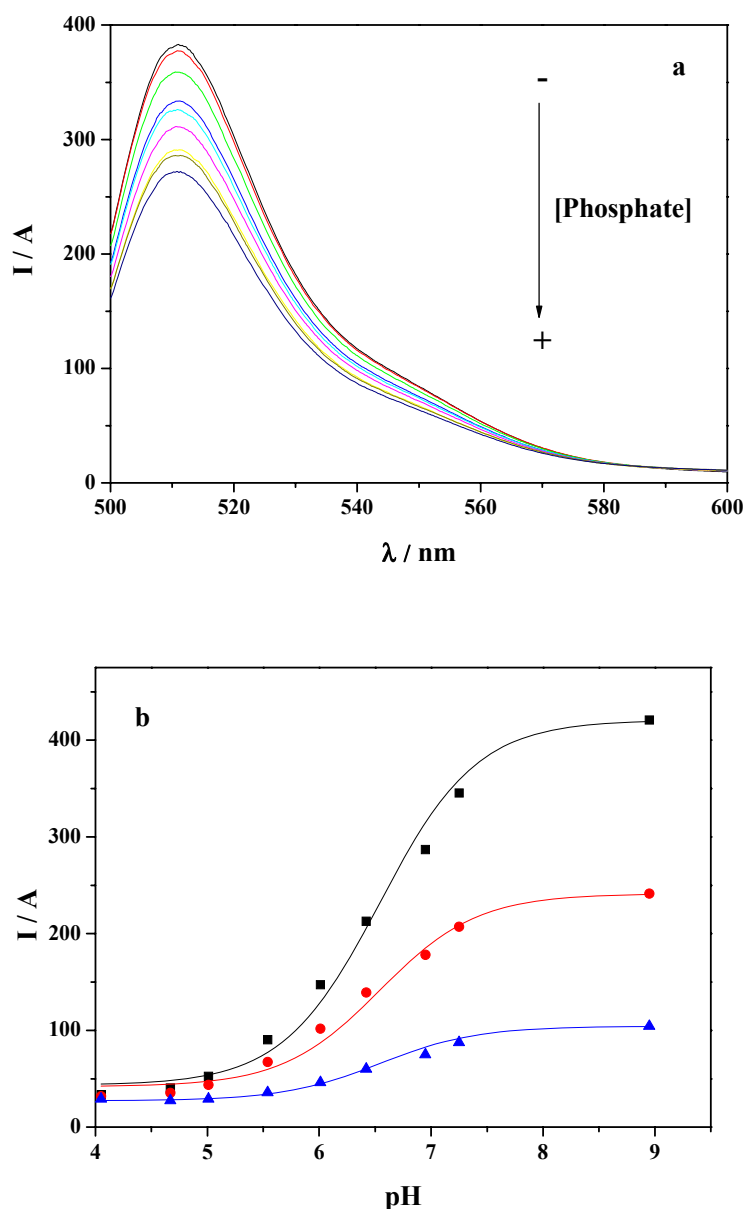


Figure S6. (a) Steady-state emission spectra ($\lambda_{\text{ex}} = 490 \text{ nm}$), normalized by the absorbance, of $4 \times 10^{-6} \text{ M}$ TG-II aqueous solutions at different phosphate buffer concentrations: 0.002 to 1 M, and pH 6.8. (b) Plot of the experimental steady-state fluorescence intensity normalized by absorbance ($\lambda_{\text{ex}} = 490 \text{ nm}$ and $\lambda_{\text{em}} = 515 \text{ nm}$ (■), 500 nm (●) and 550 nm (▲)) vs pH, from solutions of $4 \times 10^{-6} \text{ M}$ TG-II and 1.0 M phosphate buffer. Eq S4 was fitted to these experimental values. The solid lines represent the best fitting curves.

Electronic Supplementary Material for PCCP

This Journal is © The Owner Societies

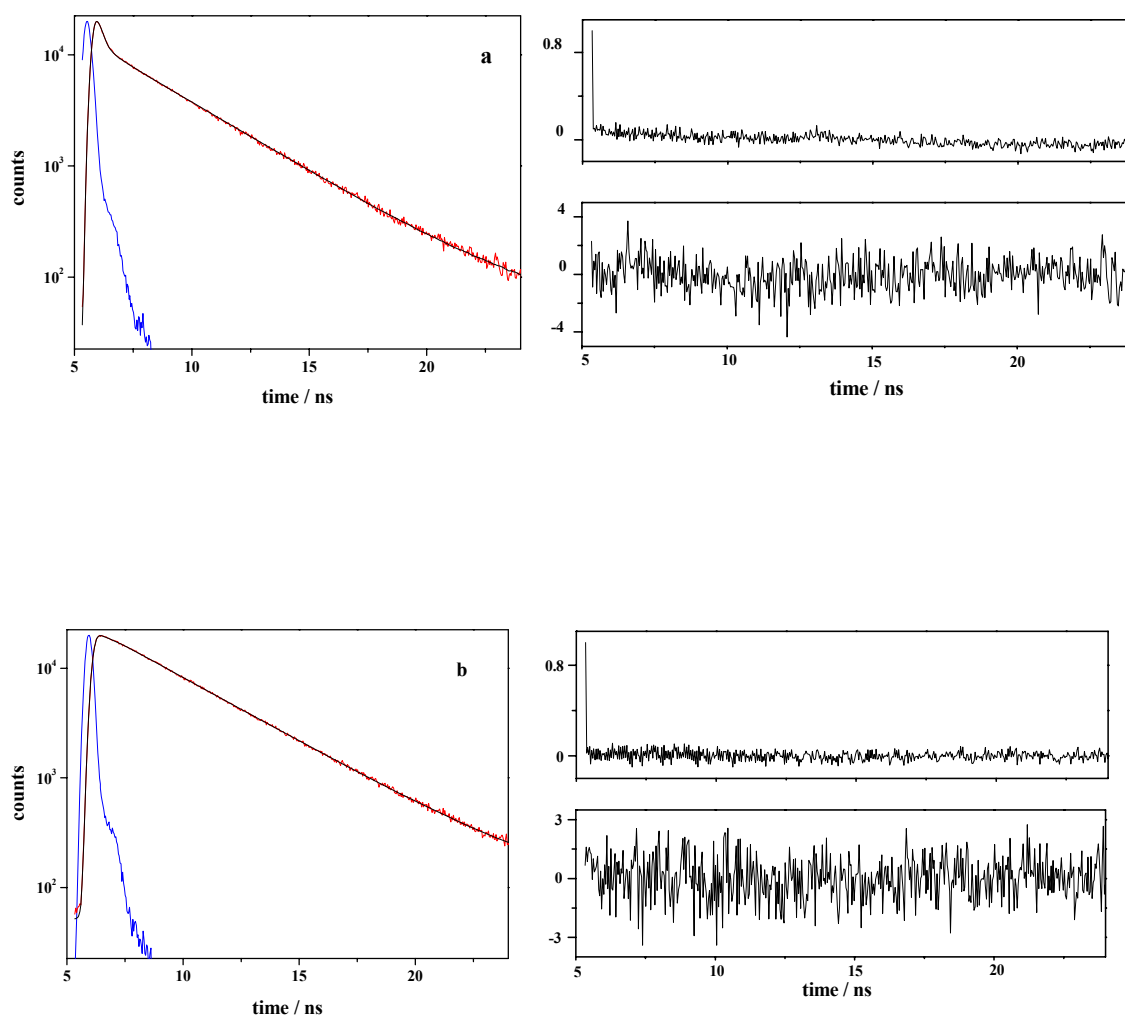


Figure S7. Fluorescence decay traces (—) of TG-II aqueous solutions ($\lambda_{\text{ex}} = 488$ nm) at (a) pH = 4.86, $C^{\text{B}} = 0.05$ M, $\lambda_{\text{em}} = 515$ nm, $\chi^2 = 1.16$; (b) pH = 6.45, $C^{\text{B}} = 0.05$ M, $\lambda_{\text{em}} = 515$ nm, $\chi^2 = 1.10$. The instrument response function (—), the fitting from GCA (—), the autocorrelation function, and the residuals, are also shown.

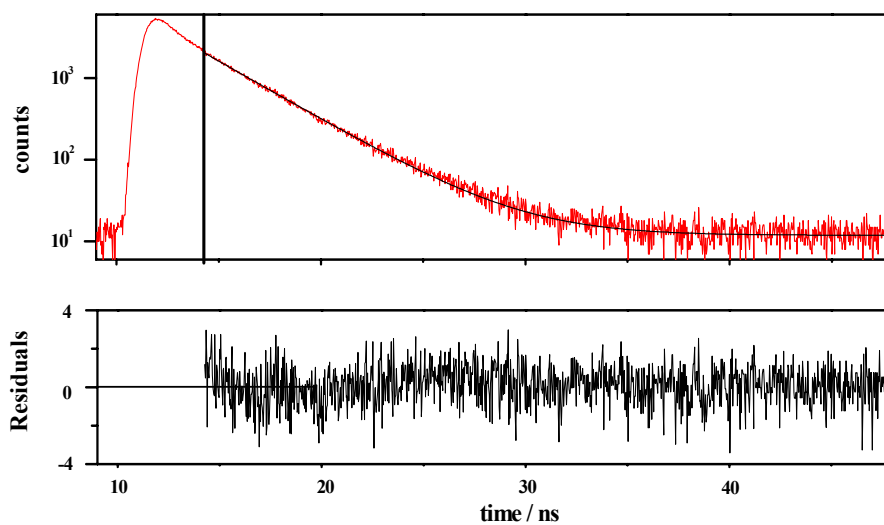


Figure S8. Fluorescence decay traces (—) at single molecule level of TG-II aqueous solution ($\lambda_{\text{ex}} = 488$ nm) at pH 6.60 and $C^{\text{B}} = 0.3$ M. The recovered lifetime was 2.99 ns, with a χ^2 of 1.21. The fitting (—) and the residuals are also shown. The fitting range started after the decay curve maximum (time gated 1.74 ns) to clip the IRF influence.